Desalination and Water Treatment
www.deswater.com

doi: 10.5004/dwt.2019.23985

152 (2019) 148–160
June

Thermo-economic modeling and multi-objective optimization of multiple-effect desalination integrated with an organic Rankine cycle

Zahra Hajabdollahi†, Kyung Chun Kim*

School of Mechanical Engineering, Pusan National University, Busan 609-735, Republic of Korea,
emails: kckim@pusan.ac.kr (K.C. Kim), zahraouderji@pusan.ac.kr (Z. Hajabdollahi)

Received 6 November 2018; Accepted 17 February 2019

ABSTRACT

This paper presents a thermo-economic model of an organic Rankine cycle (ORC) combined with a diesel engine and a multi-effect desalination (MED) technology. The heat recovered from the diesel engine is used to run the ORC for power production. The outlet vapor flow of the turbine then enters the first stage (effect) of the desalination for fresh water production. The system was optimized to maximize the total efficiency and minimize the total annual cost (TAC) of the system simultaneously. The results of the optimum designs are presented as a set of optimum points using a Pareto front. The variations of both objective functions with changes in the design parameters are presented. The evaporator pressure and partial load have the highest effect on the objective functions. The final optimal solution was obtained, and the design parameters and objective functions were calculated. The thermodynamic and economic optimum points are defined and the MED performance ratio results are compared in these two points with the results in the final optimum point. The MED performance ratio in the final optimum point was obtained to be 0.7275 and fresh water production has 183% increase in the final optimum point as compared with the economic optimum point. In addition, 3.41% increase was achieved for the thermal efficiency of the system in the final optimum point as compared with the optimum economic point, and the TAC decreases significantly as compared with the optimum thermodynamic point. Finally, the effects of the design parameters on the performance ratio, heat transfer surface area, and other factors are discussed.

Keywords: Diesel engine; Performance ratio; Total efficiency; Total annual cost; MED

1. Introduction

Less than 0.5% of available water resources is fresh water, which makes desalination a promising technology. One of the challenges that many countries are dealing with is the steady increase of freshwater demand due to the development of industry, agriculture, life standards, and population growth. In some areas, salt water is the only source of water, so it is economical to use desalination to produce fresh water. Desalination technologies are divided into two categories. Phase change occurs in processes of the first category, such as multi-effect distillation (MED), multi-stage flash distillation as well as vapor compression distillation. In the other type of desalination, the processes are performed without phase change and include reverse osmosis (RO) and electrodialysis (ED). Each desalination technology needs energy for freshwater production, which can be supplied by thermal, mechanical, or electrical energy.

MED has been used for a long time in industrial distillation. Currently, desalination is often being integrated with combined heat and power generation systems. Combined production is a process that uses the extra heat produced in electricity generation. In desalination, combined production

† Co-First Author
* Corresponding author.

means the production of fresh water from seawater or saltwater in an integrated unit where a power plant acts as a source of energy for fresh water production.

Using the recovered waste heat from different devices, the feed water flow does not need to be pre-heated [1]. The desalination systems that run by the fossil fuels are more expensive than the multi-generation desalination power plants [2]. In the thermal analysis of the desalination run by solar energy to find a proper configuration of the system, more than 25,000 m^3 d^{-1} of fresh water should be produced [3].

In the thermal analysis of two scenarios for an organic Rankine cycle (ORC) integrated with a humidification–dehumidification desalination (HDD) to obtain higher value of desalinated water, *n*-octane is considered to be the best as compared with isopentane, *n*-pentane and *n*-heptane as working fluid [4]. In the ORC system combined with HDD to investigate the system from a thermo-economic viewpoint toluene is found to be better than *n*-heptane, R600, R245fa and isopentane as the working fluid [5]. In the combination of an ORC with mechanical vapor compression desalination, the fresh water production has a peak value by the increase of the turbine inlet pressure [6].

The effects of number of stages used in multi-stage flash desalination combined with an ORC using two refrigerants: R134a and R245fa are measured by Al-Weshahi et al. [7]. It was concluded that R245fa has a better performance than R134a for their configuration. Different types of desalination including MED and RO systems have been analyzed from the exergy tools to minimize the exergy losses [8]. Exergy analysis of the MED-TVC also showed that the exergy destruction in the thermal vapor compression (TVC) unit is highest as compared with other equipment including the pumps and condenser [9]. In the techno-economic analysis of the MED and RO desalination with the low enthalpy geothermal energy, the feed water quality and desalination operational lifetimes are very important in the variation of the results and the RO unit is considered to be more cost-effective [10]. In another research, the low-cost and low-enthalpy geothermal systems for the fresh water purpose were compared with conventional system by Bundschuh et al. [11] to deliver energy efficient. Nihill et al. [12] combined a thermal water pump with a desalination unit to produce1.27 L h^{-1} of fresh water in the heat source of 86°C by the total energy of 165 MJ m^{-3}.

From the literatures, it can be found that most of the studies have been carried out in the aspect of thermal analysis, and in some cases, researchers have tried to enhance the thermal performance of the system. However, some researchers focus on the economic status of the combined ORC integrated with MED, but it was, for example, the comparison of the two systems cost, and not considering the lowest possible price for each system. In fact, by considering the thermal efficiency of the system or the fresh water production as the single function, the results are not cost-effective, because the parameters would be selected in the way that makes a significant increase in the system cost. As a result, a thermos-economic analysis of the system integrated with the MED is necessary to optimize both the thermal performance of the system as well as the system cost simultaneously.

In this study, the waste heat recovered from a diesel engine is used to run an ORC–MED with three stages to produce heat, power, and fresh water. The cost and thermal efficiency of the system are optimized as the two simultaneous objective functions. In fact, the total annual cost (TAC) of the system and system efficiency are considered two objective functions. As it was mentioned just the thermal analysis of the system cannot be enough. Just as an example if the system is supposed to maximize the fresh water production without considering the system cost, as a result more heat from the prime mover (PM) would be rejected to increase the ORC efficiency and consequently the fresh water production. Therefore, in the fixed value of the power delivered by the power plant, the PM capacity size would be selected higher to compensate the reduction of the power caused by the waste heat rejection increment. Hence, the system annual cost would be selected very high.

To avoid this problem, the TAC of the system is minimized as well as the system efficiency is maximized simultaneously. For this reason, turbine and condenser pressures, ORC mass flow rate, diesel engine capacity, and diesel engine partial load have been selected as the five decision parameters, which can be varied in their upper and lower bounds of variation. Fast and elitism non-dominated sorting approach has been applied on the simulation results to obtain the optimum solution and the programming code is written in MATLAB R2014b. Thus, the design parameters in the case of optimum solution are introduced as the best configuration for the presented system from the thermo-economic viewpoint. In addition, the most effective parameters are introduced by evaluation of the design parameters distribution vs. their indexes. Finally, the effects of design parameters including the inlet pressure of the turbine and ORC mass flow rate on the produced freshwater and other MED specifications are investigated.

2. Thermal analysis

2.1. Diesel engine

A diagram of the combined diesel ORC integrated with MED is shown in Fig. 1. The diesel engine generates power as well as some heat that is released in the form of exhaust gas, jacket water, radiation, etc. This wasted heat can be applied to run other thermodynamic systems for the power and heat generation in which only the exhaust and jacket water can be recovered and used. The equations related to the produced power and recovered heat by the diesel engine (received in the evaporator) are achieved from the curve fitting and presented below [13]:

$$\frac{\dot{Q}_w}{\dot{m}_f \mathrm{LHV}_f} = 24.01\exp\left(-0.0248\left(\mathrm{PL}\right)\right) + 15.35\exp\left(0.002822\left(\mathrm{PL}\right)\right) \quad (1)$$

where $\dot{m}_f$, LHV_f, and PL are the fuel mass flow rate, the lower heat value of fuel, and the partial load, respectively.

The power generated by the PM is defined as follows [13]:

$$\frac{\dot{W}_D}{\dot{m}_f \mathrm{LHV}_f} = 1.07\exp\left(-0.0005736\left(\mathrm{PL}\right)\right) - 1.259\exp\left(-0.05367\left(\mathrm{PL}\right)\right)\eta_{D,\mathrm{nom}} \quad (2)$$

where $\eta_{D,\,\mathrm{nom}}$ is the nominal efficiency of the diesel engine. The mass flow rate of the fuel from the diesel engine with the

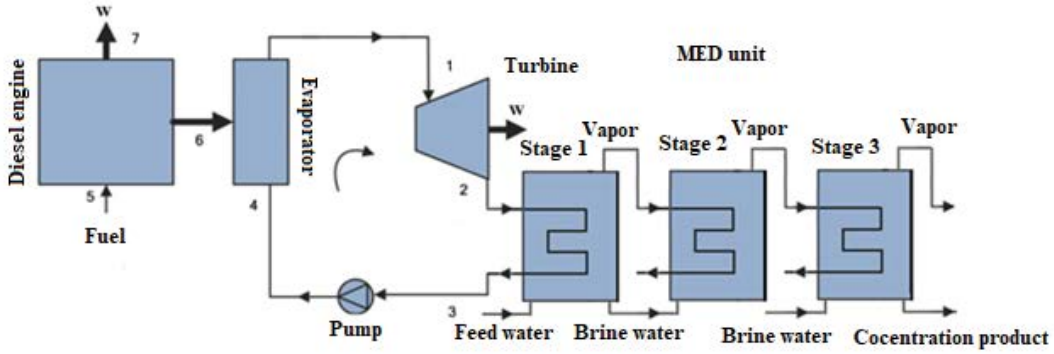

Fig. 1. Diagram of the ORC integrated with MED.

nominal efficiency of 35% can be expressed as a function of the partial load as follows [13]:

$$\frac{\dot{m}_f}{\dot{m}_{f,\text{nom}}} = 0.02836\exp\left(0.03254\left(\text{PL}\right)\right) + 0.02556\exp\left(0.01912\left(\text{PL}\right)\right) \tag{3}$$

where $\dot{m}_{f,\text{nom}}$ is the consumed fuel in the nominal capacity of diesel engine as follows:

$$\dot{m}_{f,\text{nom}} = \frac{\dot{W}_D}{\eta_{D,\text{nom}}\text{LHV}_f} \tag{4}$$

2.2. Turbine

Vapor enters the turbine at point 1 as it can be seen in Fig. 1. The power generated in the turbine is equal to:

$$\dot{W}_T = \eta_T \dot{W}_{T,s} \tag{5}$$

The turbine efficiency can be obtained by:

$$\eta_T = \frac{h_1 - h_2}{h_1 - h_{2,s}} \tag{6}$$

2.3. Pump

The real pump power in steady-state condition is obtained below by neglecting the heat loss and using the definition of isentropic efficiency:

$$\dot{W}_P = \frac{\dot{W}_{P,s}}{\eta_P} \tag{7}$$

$$\eta_P = \frac{h_4 - h_{5,s}}{h_4 - h_5} \tag{8}$$

The pump outlet properties can be obtained using the inlet properties, isentropic efficiency, and pump outlet pressure.

2.4. MED

Desalination is used to purify seawater for drinking purposes. Generally, a desalination system divides saline water into two streams: pure water with a very small percentage of salt and another stream that contains the residual salt which is called brine. In MED, the outlet stream from the power plant first enters the first stage of desalination. In fact, the vapor from the turbine enters the first stage as the hot stream. The feed water is sprayed over the tubes containing the hot stream. Therefore, a part of the feed water is converted to the vapor and used as the hot stream for the second stage. The remaining of the feed water (brine produced in the first stage) enters the second stage as the secondary feed water flow, and the process is repeated for each stage.

By considering the mass balance for the MED, we have:

$$\dot{m}_f = \dot{m}_{v1} + \dot{m}_{v2} + \dot{m}_{v3} + \dot{m}_P \tag{9}$$

where $\dot{m}_f$, $\dot{m}_v$, and $\dot{m}_p$ are the mass flow rate of the feed water, the vapor mass flow rate from each stage, and the concentrated product (the brine produced in the last stage) mass flow rate, respectively. The subscripts 1, 2, and 3 are represented for each stage of MED in the all equations of this section. The mass balance can be expressed as follows:

$$x_f \dot{m}_f = x_P \dot{m}_P \tag{10}$$

x_f and x_P are the salt fractions in the feed stream and concentrated product stream, respectively. The enthalpy balance for each stage of MED is calculated as follows:

$$\begin{aligned}
&\dot{m}_f H_f + \dot{m}_s H_{vs} = \dot{m}_{v1} H_{v1} + \dot{m}_{f1} H_{f1} + \dot{m}_s H_{cs} \\
&\dot{m}_{f1} H_{f1} + \dot{m}_{v1} H_{v1} = \dot{m}_{v2} H_{v2} + \dot{m}_{f2} H_{f2} + \dot{m}_{v1} H_{cs1} \\
&\dot{m}_{f2} H_{f2} + \dot{m}_{v2} H_{v2} = \dot{m}_{v3} H_{v3} + \dot{m}_P H_{P3} + \dot{m}_{v2} H_{cs2}
\end{aligned} \tag{11}$$

where H_{vs}, H_v, H_f, and H_{cs} are the enthalpy of the saturated steam (which can be obtained from a steam table), the enthalpy of the vapor from each stage, the enthalpy of the concentrated product stream leaving each stage, and the condensate's stream enthalpy, respectively. The mass balance, solid balance, and enthalpy balance equations give us five

equations that are solved simultaneously. The temperature difference between the two stages is [14]:

$$\Delta T = T_1 - T_2 \tag{12}$$

Here it should be mentioned that the subscripts 1 and 2 are related to the MED part not ORC. The brine temperature for each stage can be obtained as follows [14,15]:

$$T_i = T_{vi} + \text{BPE} \tag{13}$$

T_{vi} is the temperature of the vapor produced in stage *i*, and BPE is the boiling point elevation [16]:

$$\text{BPE} = x\left(\text{A} + \text{B}x + \text{C}x^2\right) \tag{14}$$

where x is the solid fraction, and the coefficients A, B, and C are calculated as follows [17]:

$$\text{A} = \left(8.325\times10^{-2} + 1.883\times10^{-4}T + 4.02\times10^{-6}T^2\right) \tag{15}$$

$$\text{B} = \left(-7.625\times10^{-4} + 9.02\times10^{-5}T - 5.2\times10^{-7}T^2\right) \tag{16}$$

$$\text{C} = \left(1.522\times10^{-4} - 3\times10^{-6}T - 3\times10^{-8}T^2\right) \tag{17}$$

For the heat transferred in each stage, we have:

$$\begin{aligned} q_1 &= U_1A_1\left(T_s - T_1\right) = \dot{m}_sH_{vs} - \dot{m}_sH_{cs} \\ q_2 &= U_2A_2\left(T_{v1} - T_2\right) = \dot{m}_{v1}H_{v1s} - \dot{m}_{v1}H_{cs1} \\ q_3 &= U_3A_3\left(T_{v2} - T_3\right) = \dot{m}_{v2}H_{v2s} - \dot{m}_{v2}H_{cs2} \end{aligned} \tag{18}$$

U, A, and T are the overall heat transfer coefficients, heat transfer area of each stage, and the temperature of each stage. Subscripts s, v, and cs are related to the hot vapor stream coming to the stage, vapor produced in each stage and concentrated stream produced in each stage.

The proportion of fresh water produced with respect to the vapor (or steam in the case of water) consumed is the thermal performance ratio of desalination:

$$\text{PR} = \frac{m_D}{m_s} \tag{19}$$

m_D is the fresh water produced in the all stages which is the sum of vapor produced in each stage (or desalinated mass flow rate). m_s is the mass flow rate of the hot stream which enters to each stage which is considered to be the vapor of R245fa in the first stage and is the steam in the second and third stages.

2.5. Total cycle

The total power obtained from the cycle including the ORC and the diesel engine is expressed as follows:

$$\dot{W}_{\text{tot}} = \dot{W}_{\text{PM}} + \dot{W}_{\text{net,ORC}} \tag{20}$$

where $\dot{W}_{\text{PM}}$ is the power obtained by the diesel engine, and $\dot{W}_{\text{net,ORC}}$ is the total power achieved by the ORC, which is the difference in power consumed by the pump ($\dot{W}_P$) and power generated by turbine ($\dot{W}_T$).

$$\dot{W}_{\text{net,ORC}} = \dot{W}_T - \dot{W}_P \tag{21}$$

The total efficiency of the system is defined as:

$$\eta_{\text{tot}} = \frac{\dot{W}_{\text{tot}}}{\dot{m}_{f-\text{PL}}\text{LHV}} \tag{22}$$

where $\dot{m}_{f-\text{PL}}$ is the fuel required for the diesel engine, and LHV is the lower heat value of the fuel.

3. Economic modeling of the system

The TAC of the system is considered to be one of the objective functions, which should be minimized. The TAC includes the investment cost of the system, fuel cost, and cost related to the system emission:

$$\text{TAC}\left(\frac{\$}{\text{year}}\right) = \alpha\beta C_{\text{inv}} + C_{\text{fuel}} + C_{\text{em}} \tag{23}$$

α is the annual factor, and β is the maintenance factor, which is defined as follows:

$$\alpha = \frac{i}{1-\left(1+i\right)^{-n}} \tag{24}$$

i is the interest rate of the system and n is the life time.

In Eq. (25), the investment cost includes the cost of each equipment used in the system. The equipment is included in the price of the diesel engine, turbine, evaporator, MED, and pump.

$$\begin{aligned} C_{\text{inv}} &= C_{\text{inv},T} + C_{\text{inv,MED}} + C_{\text{inv},D} + C_{\text{inv},P} + \\ C_{\text{inv,ev}} &= a_1(\dot{W}_T)^{b_1} + a_2(A_{\text{MED}})^{b_2} + a_3(\dot{W}_D)^{b_3} + a_4(\dot{W}_P)^{b_4} + a_5(A_{\text{ev}})^{b_5} \end{aligned} \tag{25}$$

A_{MED} is the total heat transfer area of the desalination stages. The coefficients a_1–a_5 and b_1–b_5 are used to consider local costs.

The fuel cost in the equation above is expressed as follows:

$$C_{\text{fuel}} = \left(\dot{m}_{f,D}\times3{,}600\right)N\phi_f \tag{26}$$

The emission cost is:

$$C_{\text{em}} = \left(\dot{m}_{\text{CO}_2}\times3{,}600\right)N\psi_{\text{em}} \tag{27}$$

where N, ϕ_f, $\dot{m}_{\text{CO}_2}$, and ψ_{em} are the operational hours of the system in a year, the unit price of fuel, fuel mass flow rate, and the penalty cost for the produced emission ($\$\ \text{kg}^{-1}$), respectively.

4. Objective functions, design parameters, and constraints

The selected objective functions to be optimized are the TAC of the system and system efficiency (PM and ORC). The TAC of the system is minimized, and the efficiency is maximized simultaneously. Five design parameters are used in the optimization: the nominal capacity of the diesel engine, partial load, evaporator pressure, condenser pressure, and ORC mass flow rate. The design parameters and their ranges of variation are listed in Table 1.

The constraints considered for the optimization algorithm are the following:

- The inlet temperature of the condenser should be higher than 45°C to keep the condenser temperature above the ambient temperature.
- The vapor quality of the turbine outlet should be higher than 0.95% to prevent the turbine blade from corroding.
- The evaporator pressure should be higher than the condenser pressure ($P_1 > P_2$).

Subscripts 1 and 2 are presented for the ORC system. Usually, two or more functions that are typically in conflict with each other are optimized simultaneously in multi-objective optimization problems [13]. It means when one objective is improved, the other objective is ruined. Therefore, a set of conflicting optimum solutions is selected as a Pareto optimal front. The multi-objective optimization is defined as follows:

Find $X = \left(X_i\right) \quad \forall i = 1,2,...,N_{\mathrm{dp}}$

where $f_j(X)$ is the objective function to be optimized $\forall j = 1,2,...,M_{\mathrm{obj}}$

by considering the two constraints as follows:

$$g_k\left(x\right) = 0 \qquad \forall k = 1,2,...,K \tag{28}$$

$$h_z\left(x\right) \le 0 \qquad \forall z = 1,2,...,Z \tag{29}$$

In these equations X, f, g, and h are the decision variables, objective functions, and equal and unequal constraints, respectively. N_{dp}, M_{obj}, K, and Z are the number of decision variables, number of objective functions, number of equal constraints, and number of unequal constraints, respectively. Deb's definition is used for the solution ranking [18]. A set of non-dominated points is considered to create the Pareto front solutions. When the two objective functions are in conflict, the Pareto front has the form of two-dimensional lines, and when there are three conflicting objectives, the form is a surface [19].

Table 1
Design parameters and their lower and upper bounds of variation

Variables	Lower bound	Upper bound
P_1 (kPa)	100	2,000
P_2 (kPa)	50	2,000
ORC mass flow rate (kg s^{-1})	0.1	5
Partial load (%)	0	50
Nominal capacity (kW)	100	200

5. Case study

R245fa has been selected as the working fluid for this study since its critical temperature (154°C) is higher as compared with the cases of most other common working fluids including R123, R22 R134a, etc. From the other hand, the evaporator temperature is higher than the critical temperature of mentioned common working fluid except R245fa. The design parameters are considered to be for a place with ambient temperature of 25°C. The equations governed on the system have been solved by a code written in MATLAB 2014b. The depreciation time, interest rate as well as the pollution cost of CO_2 are assumed to be 20 years, 0.12, and 0.02098 \$ kg^{-1}, respectively. The power plant is supposed to deliver 200 kW and operate for 6,000 h $year^{-1}$. The other parameters considered for the case study are listed in Table 2. Since the cost of evaporator is included in the diesel engine cost, thus the constants a_5 and b_5 are not required.

The validation of the results in the current study are compared with the results presented in the previous literature [20] in which the temperature and salt concentration in the stages 1, 2, and 3 are 92.6°C, 84.96°C, 76.84°C and 45,079, 48,612, 52,705 ppm, respectively. Khalilzadeh and Nezhad [20] applied the wind turbine as the prime mover. Since the diesel engine has been considered as the prime mover in the present study and wind turbine in the reference, as a result the associate waste heats in two different wind speeds of 8 and 9 m s^{-1} are considered in Table 3 which are equal to 122 and 155 kW, respectively. In fact, just the vapor production in the three stages of the MED can be enough for our validation, since the other features of MED are dependent on the vapor mass flow rate production. As a result, the calculation of the vapor produced in the three stages of MED are compared. The overall heat transfect coefficient for the first stage is considered to be 2.4 kW/m^{-2}°C by the temperature difference of 60°C between the first and last stages of the MED unit. In addition, the seawater temperature and inlet pressure were considered to be 25°C and 200 kPa, respectively, for the validation. By looking at the results listed in the table, the accuracy of the present simulation can be approved.

Table 2
Input parameter

Parameters	Values
Isentropic efficiency of the pump	0.9
Isentropic efficiency of the turbine	0.9
Nominal efficiency of the diesel engine	35%
Diesel fuel cost (\$ kg^{-1})	0.168
a_1, a_2, a_3, a_4	1,763, 4,750, 150, 3,500
b_1, b_2, b_3, b_4	0.95, 0.75, 0.8, 0.47,
ϕ	1.05
Evaporator pressure drop	5%

Table 3
Comparison of the present study results with reference [15]

	Present study	Reference [15]	Present study	Reference [15]
	Waste heat of 122 kW	Waste heat of 122 kW	Waste heat of 155 kW	Waste heat of 155 kW
Vapor production in stage 1 (kg s^{-1})	0.0354	0.0373	0.0466	0.0474
Vapor production in stage 2 (kg s^{-1})	0.0341	0.0364	0.0437	0.0463
Vapor production in stage 3 (kg s^{-1})	0.0335	0.0356	0.0426	0.0452

6. Results and discussion

Fig. 2 shows the variation of TAC vs. the total efficiency of the system. As the efficiency increases, the TAC increases, which is not desired. When improving one objective, the other objective suffers. As a result of the conflict between the two objective functions, a multi-objective optimization is required to maximize the total efficiency of the system and minimize the TAC simultaneously. The Pareto front is a set of solutions from which a designer can select a final answer. The ideal point in the diagram is where the total efficiency is highest and the TAC is lowest (the thermo-economic optimum point).

The Pareto front is divided into different parts by five points, as shown in Fig. 2. In fact, it the points are selected from various range of efficiency and TAC, in which the points between A and B have the highest efficiency and TAC, the points between B and D have the mediocre magnitude of the two objectives and finally the points between D and E have the low magnitude of both efficiency and TAC. If the system were being optimized from only a thermodynamic point of view, point A can be the solution. In contrast, point E represents the lowest cost and the lowest efficiency and can be chosen from an economic point of view. However the efficiencies at the points selected between B and C are lower than the points between A and B, but a considerable decrease can be seen in the TAC as compared with the points between A and B. The associated objective functions as well as the design parameters for these five selected points on the Pareto front are listed in Tables 4 and 5. Although 9.92% increase can be obtained in the optimum thermodynamic point (A), but the increase of the TAC should be taken into account which is significantly very high in comparison with the optimum economic point. Therefore, none of these points (optimum thermodynamic and economic points) can be considered as the final solution. By selection of point C in the mediocre range of the TAC vs. the thermal efficiency, a 0.99% decrease and 8.85% increase can be seen in the thermal efficiency as compared with the optimum thermodynamic and economic points, respectively. As a result, a significant increase of thermal efficiency can be obtained in the point C as compared with the optimum economic point. However, the TAC in the case of point C is higher than the optimum economic point TAC, but it is not that much high in comparison with the optimum thermodynamic point TAC. Therefore, the final optimum answer can be found as a point in the neighbor of point C in which is calculated in details in the section 7.

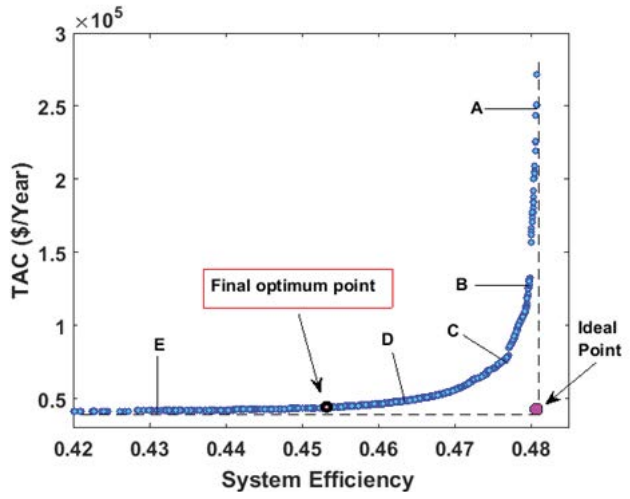

Fig. 2. Objective function Pareto front.

Fig. 3 shows the distribution of each design parameter vs. their index in the population through the lower and upper bounds of variation for the optimum points. The upper and lower bounds of variation for each design parameter are represented by dotted lines. There is an equal distribution of the optimum points in the case of the evaporator pressure and partial load through the upper and lower bounds of variation, as shown in Figs. 3(a) and (d). In the allowable range of variations for the ORC mass flow rate and condenser pressure, a semi-scattering distribution is obtained, as shown in Figs. 3(b) and (c).

The evaporator pressure and partial load have greater effects in the conflict between the two objective functions at the optimum points. The mass flow rate of the ORC cycle has been selected to be lower than 2 kg s^{-1}. At higher ORC mass flow rates, the condenser temperature can be reduced, so the constraints in Section 4 will not be satisfied (Fig. 3(b)). In the

Table 4
Values of the objective functions at the selected points of the Pareto front

	A	B	C	D	E
Efficiency (%)	0.4808	0.4799	0.4761	0.4619	0.4374
TAC ($ $year^{-1}$)	3.602e+05	1.324e+05	0.752e+05	0.476e+05	0.431e+05

Table 5
Values of the design and desalination parameters at five selected points on the Pareto front

Design parameters	Point A	Point B	Point C	Point D	Point E
P_1 (kPa)	974.12	974.08	99.83	1,156.67	879.1
P_2 (kPa)	295.1	305.4	339.64	103.2	103.6
ORC mass flow rate (kg s^{-1})	1.81	1.85	1.47	0.4	0.41
Partial load (%)	95.8	95.56	70.00	56.40	50.12
Nominal capacity (kW)	100.00	100.02	100.02	100.00	100.05
Performance ratio	0.0022	0.0024	2.3625	1.102	0.5321
Vapor production in the stage 3 (kg h^{-1})	5.4450e+03	5.5587e+03	4.2437e+03	818.2494	705
Vapor production in the stage 2 (kg h^{-1})	5.4061e+03	5.5208e+03	4.1592e+03	566.7906	216
Vapor production in the stage 1 (kg h^{-1})	5.3344e+03	5.4492e+03	4.1579e+03	371.0721	143
Mass fraction in the stage 1 (%)	0.3931	0.3956	0.3659	0.3049	0.2981
Mass fraction in the stage 2 (%)	0.5680	0.5788	0.4695	0.3128	0.3009
Mass fraction in the stage 3 (%)	0.6825	0.692	0.6547	0.3248	0.3105
Performance ratio	2.4819	2.4805	2.3625	1.1017	0.5321

case of the diesel engine capacity, a semi-intensive distribution can be seen in the selected range of variation, as shown in Fig. 3(e). When increasing the diesel capacity, the power produced by the engine increases, which leads to a decrease in the heat recovered by the ORC and the ORC efficiency.

In contrast, when decreasing the diesel capacity, the rejected heat increases since the engine efficiency decreases, which causes an increase in the ORC efficiency. As a result, the diesel engine capacity should be selected in the range in which the constraints in Section 4 are satisfied, and a higher total system efficiency can be achieved. An optimal value can be obtained for the diesel engine where both the highest diesel engine and highest ORC efficiency are calculated.

Fig. 4 shows the effects of the design parameters on the TAC and total efficiency of the system at five particular optimum design points. The first point in the diagrams is where the Pareto related to point A dominates over the other Pareto points in the higher range of efficiency. This means at higher efficiency, the points selected on Pareto front A have lower TAC at a fixed efficiency. In addition, at lower efficiency (less than 0.462), Pareto front E dominates, which means the points selected on this Pareto front have the lowest TAC compared with other Pareto fronts at a fixed value of efficiency.

TAC and the system efficiency are increased as the evaporator pressure increases, as shown in Fig. 4(a). However, as the evaporator pressure increases, the turbine inlet and outlet enthalpy decrease, but the total difference between them increases due to the enhancement of the turbine power. Moreover, when the evaporator pressure increases, the power required for the pump increases. Because the turbine generated power is dominant, the system efficiency improves. Furthermore, the investment cost of the turbine, pump, and MED increases with the increase of the evaporator pressure, which causes an increase in TAC.

With the increase of the mass flow rate, both the system efficiency and TAC increase because higher power can be generated by the turbine, which leads to an increase in efficiency (Fig. 4(b)). With an increase in the ORC mass flow rate, the investment cost increases due to the increase of the equipment cost for the turbine, pump, and desalination. This occurs because the increase of the mass flow rate results in the requirement of a higher heat transfer surface area in the desalination stages with a fixed amount of desalinated products.

With an increase of the turbine outlet pressure, the total system efficiency and TAC decreased, as shown in Fig. 4(c). The useful energy produced from the pressure difference in the turbine is reduced, and thus, at a fixed value of the diesel engine power, the total efficiency of the system is decreased. In contrast, the TAC decreases when there is a decrease of the power in the turbine and pump and the MED heat transfer area. Because of the higher temperature of the flow to the MED, a lower surface area is needed for each stage.

With an increase of the partial load, the efficiency and TAC decrease at all selected optimal design points, as shown in Fig. 4(d). The mass flow rate of the fuel from the diesel engine increases due to the increase of the partial load, and consequently, the total system efficiency decreases. However, the fuel cost and pollution cost increase, but the increase of the heat source temperature causes a decrease in the heat transfer area of the MED, and the total cost of the system decreases.

With an increase of the diesel capacity, the total efficiency of the system decreases, as shown in Fig. 4(e). The fuel consumed by the diesel engine is increased by the increase of the diesel capacity, which has a negative effect on the system efficiency. The TAC is first decreased and then increased by the variation of the diesel capacity. The heat transfer area decreases due to the decrease in the cost because of the high temperature of the inlet vapor to the first stage of the MED.

With an increase of the diesel capacity, the fuel cost and the pollution cost increased and dominated over the cost of the MED heat transfer area. As a result, an optimal point can be found for the capacity of the diesel engine at which the TAC is lowest and is obtained around 100. This is the reason for the semi-intensive distribution in the vicinity of the optimal capacity (Fig. 3(e)).

Fig. 5 shows the effects of the evaporator pressure on the different parameters of the MED. The variation of the evaporator pressure on the solid mass fraction in the third stage

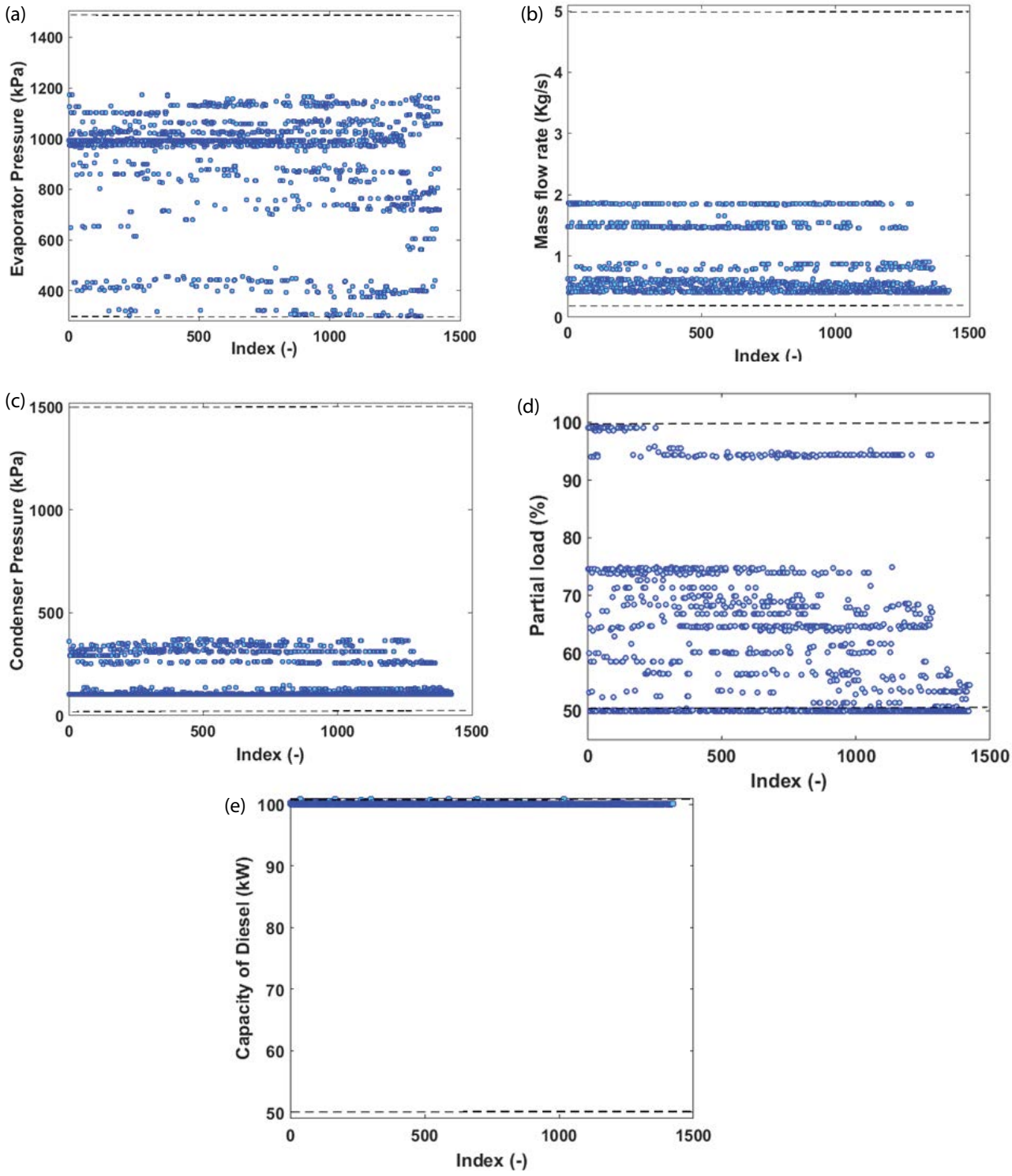

Fig. 3. Distribution of design parameters in their range of variation vs. the population index. (a) Evaporator pressure, (b) ORC mass flow rate, (c) condenser pressure, (d) partial load, and (e) diesel engine capacity.

is shown in Fig. 5(a). With the increase of the evaporator pressure, the inlet temperature to the first stage of the MED decreases, which causes an increase in the value of the vaporized product. This means that more feed water is vaporized, and the ratio of the solid fraction to the feed water increases (or mass concentration (ppm) × 10^{-6}).

Point A in the Pareto front has the highest efficiency and thus the lowest condenser temperature, which leads to a

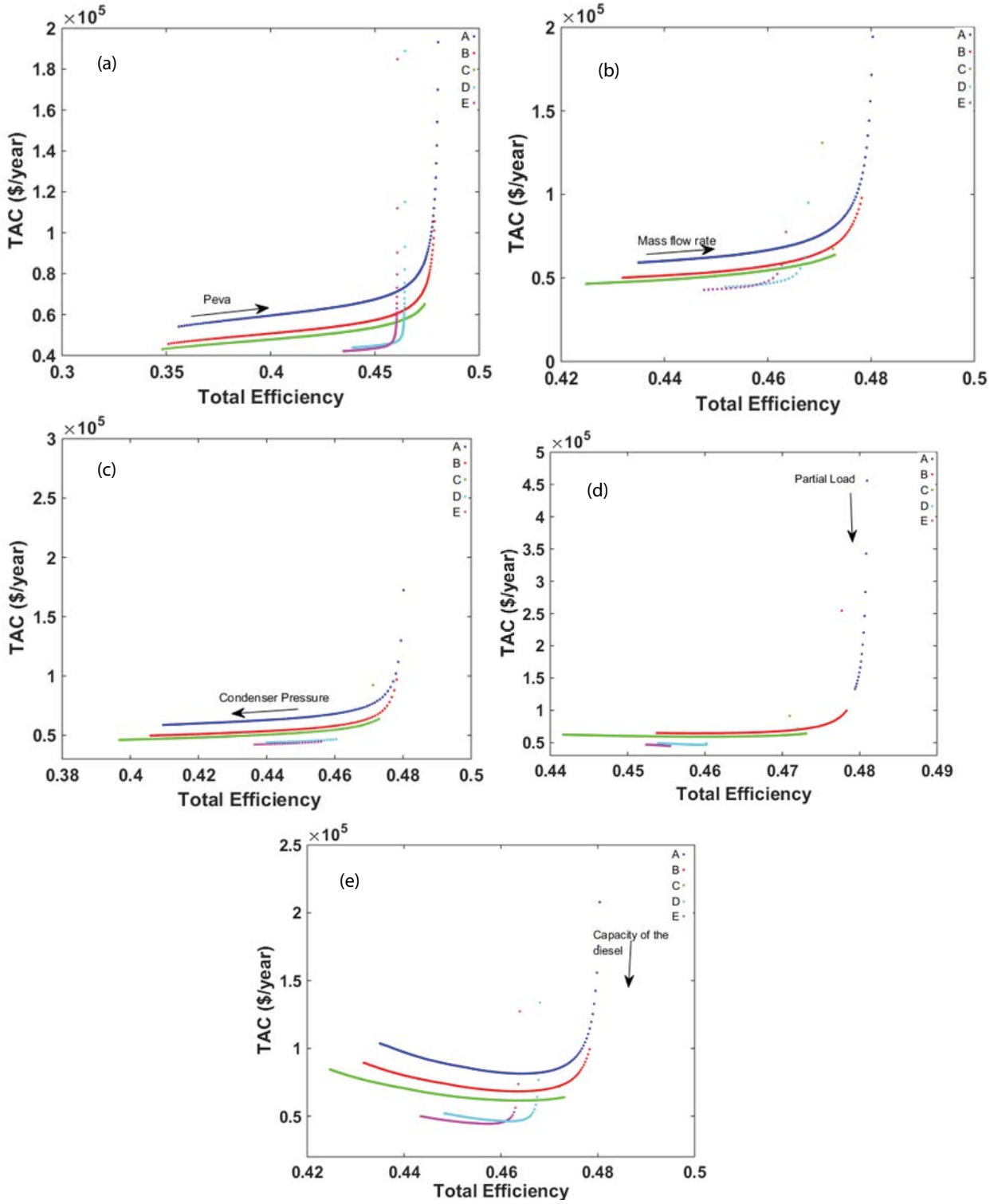

Fig. 4. TAC Pareto front vs. the total efficiency at five particular points shown in Fig. 2 for different design parameters. (a) Evaporator pressure, (b) ORC mass flow rate, (c) condenser pressure, (d) partial load, and (e) diesel engine capacity.

higher vapor production and solid mass fraction than at other points. As a result, at a fixed value of the ORC mass flow rate, the performance ratio is increased and has the highest value in the Pareto front related to point A, as shown in Fig. 5(b). There is an opposite trend in the case of brine water production produced in each stage, as shown in Fig. 5(c). This occurs because with the increase of vapor production, a lower amount of the heat remains for the production of brine water.

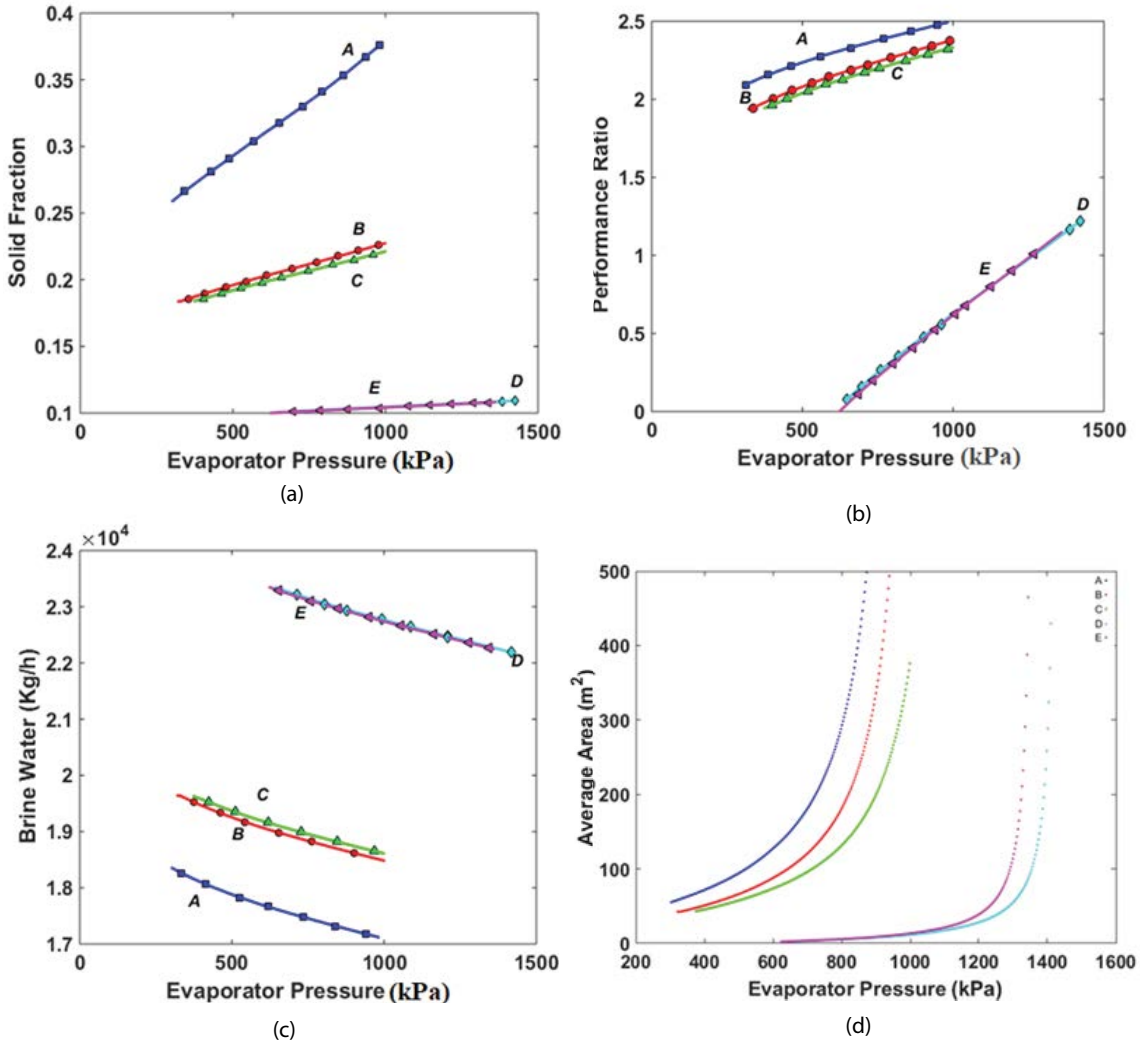

Fig. 5. Effects of evaporator pressure and ORC mass flow rate on the different parameters of MED for the five particular points shown in Fig. 2. (a) Solid fraction, (b) performance ratio, (c) brine water, and (d) average area of the stages.

As mentioned, the vapor production increases with the increase of the evaporator pressure. Therefore, at a fixed value of the ORC mass flow rate, the performance ratio is enhanced. With a decrease of the inlet temperature in the first stage of the MED (because of the increase in the evaporator pressure), a higher heat transfer surface area is needed for each stage, as shown in Fig. 5(d).

Fig. 6 shows the variation of the desalinated mass flow rate vs. the ORC mass flow rate. With the increase of the ORC mass flow rate, the flow temperature in the condenser is reduced, which increases the vapor production in the three stages. The Pareto front regarding point A has a higher mass flow rate and lower temperature, followed by Pareto fronts B, C, D, and E. As a result, the highest desalinated mass flow rate can be seen in Pareto front A.

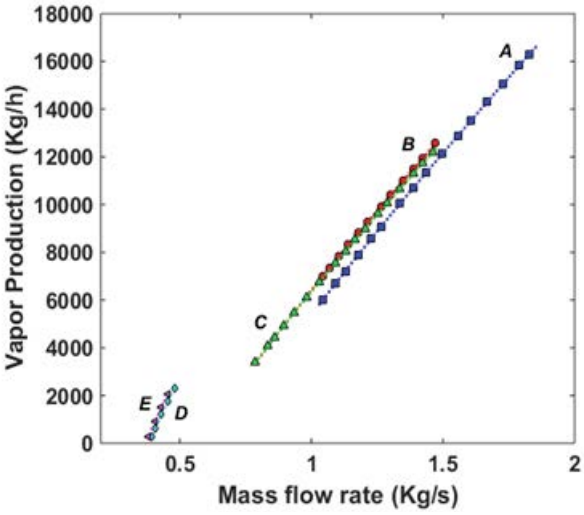

Fig. 6. Fresh water variation vs. the ORC mass flow rate at the five particular points selected in Fig. 2.

7. Selection of final optimum point

This section presents the definition of the final optimum point. The closest point to the ideal point (Fig. 2) on the Pareto front can be introduced as the final solution. The

distance of the points on the Pareto front to the ideal point can be calculated by the LINMAP method as follows [21,22]:

$$d_i = \sqrt{\sum_{j=1}^{2}\left(F_{ij}^{n} - F_{\text{ideal},j}^{n}\right)^2} \tag{30}$$

where

$$F_{ij}^{n} = \frac{F_{ij}}{\sqrt{\sum_{i=1}^{n}\left(F_{ij}\right)^2}} \tag{31}$$

In this relation, i is the index of each point on the Pareto front, j is the objective function index, and n is the total number of points in the Pareto front.

Fig. 2 shows the final optimum solution on the Pareto front and its properties are listed in Table 6. In Fig. 7, the variation of each MED stage vs. the performance ratio is graphed in the final optimum point. When the performance ratio increases with a fixed rate of fresh water production, the inlet mass flow rate to the MED (the ORC mass flow rate) decreases, which causes a lower production of vapor in each stage. To maintain a constant rate of fresh water production, more water should be evaporated through the stages. As a result, a larger surface area is required.

Table 6
Design parameters, objective functions and performance ratio at the final optimum point

Parameters	Value
Diesel capacity (kW)	100.00
Partial load (%)	50.00
Turbine inlet pressure (kPa)	1,000.30
Turbine outlet pressure (kPa)	103.20
ORC mass flow rate (kg s^{-1})	0.40
Total efficiency (%)	45.23
TAC ($ $year^{-1}$)	43,801
Performance ratio	0.7275

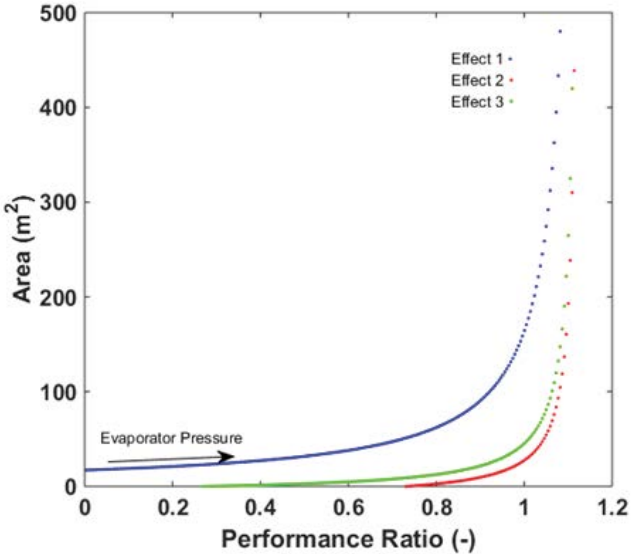

Fig. 7. Trend of heat transfer area of the three stages vs. the performance ratio with changing evaporator pressure at the final optimum point.

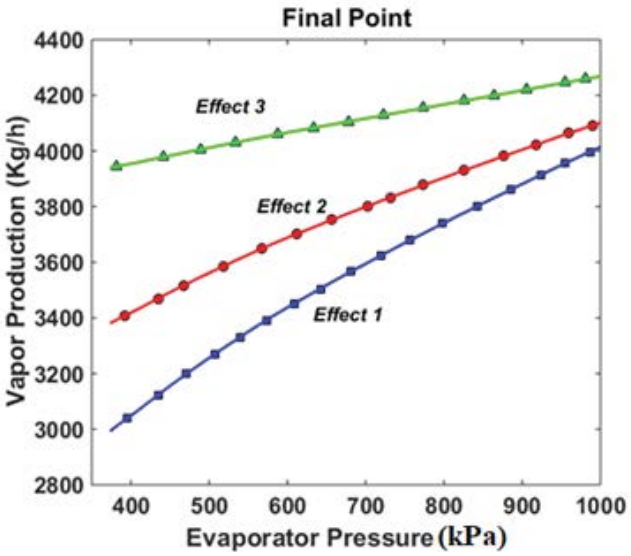

Fig. 8. Distilled product variation vs. the evaporator pressure at the final optimum point.

Fig. 8 shows the variation of the vapor production in each stage vs. the evaporator pressure to find the final optimal point. The vapor production (the distillate product) in the third stage is the highest, followed by stage 2 and stage 3. The reason is that more heat is required to heat the feed water flow (seawater) in the first effect, and by passing through the stages, the water flow becomes warmer. In the third stage, a lower amount of heat is needed to increase the water temperature. Therefore, a higher amount of received heat is used for the water vaporization in the third stage. The performance ratio in the final optimum point is obtained to be 0.7275. It is worth mentioning that the fresh water production has 183% increase in the final optimum point as compared with the economic optimum point. In addition, 3.41% increase is shown for the system thermal efficiency in the final optimal point in comparison with the optimal economic point while only 1.63% increment happens for the TAC in this point as compared with the optimal economic point. Although 6.3% increment can be seen in the thermal efficiency of the system in the optimal thermodynamic point, but the TAC increases dramatically in this case as compared with the final optimal point.

8. Conclusion

This study presented the design and modeling of a diesel engine combined with an ORC. MED was used for the fresh water production. Multi-objective optimization was applied to maximize the efficiency and fresh water production while the TAC of the system was simultaneously minimized. Five design parameters were selected: the evaporator pressure,

ORC mass flow rate, partial load, nominal capacity of the diesel engine, and the inlet pressure of the vapor to the first stage of MED. The following conclusions can be inferred from the study:

- Both TAC and the total efficiency increased with the increase of the evaporator pressure and the ORC mass flow rate.
- The TAC decreased while the total efficiency decreased with the increase of the outlet pressure of the turbine, partial load, and diesel engine capacity.
- The increase of the evaporator pressure improves the total efficiency of the system and the performance ratio of the MED, which caused an increase in the amount of fresh water.
- The ORC mass flow rate had a positive effect on the fresh water production where the increase of the ORC mass flow rate increased the vapor production in each stage.

With the increase of the evaporator pressure, the TAC increased. For this reason, a final optimum point was presented where the TAC decreased about 72.2% in comparison with the best thermodynamically optimized point (A). In comparison with the best economically optimized point (E), the ideal point showed a 3.88% increase in the total efficiency and a 1.1% increase in the TAC. Performance ratio of the MED increased 192% as compared with the economic optimum point (E). Although the performance ratio was lower in comparison with the thermodynamic optimum point (A), TAC dramatically decreased in the case of final optimum point.

Symbols

A	—	Heat transfer surface area, m^2
BPE	—	Boiling point elevation
C_{min}	—	Minimum of total heat capacity, kJ kg^{-1}K^{-1}
C_{inv}	—	Investment cost, \$
C_{fuel}	—	Fuel cost, \$ year^{-1}
C_{em}	—	Emission cost, \$ year^{-1}
H	—	Enthalpy
h	—	Specific enthalpy, kJ kg^{-1}
ir	—	Interest rate
LHV	—	Lower heating value, kJ kg^{-1}
$\dot{m}$	—	Stream flow rate, kg s^{-1}
n	—	System life time
P	—	Pressure, bar
PM	—	Prime mover
$\dot{Q}$	—	Heat transfer rate, kW
T	—	Temperature, K
U	—	Overall heat transfer coefficient
$\dot{W}$	—	Power, kW
x	—	Solid or salt fraction
TAC	—	Total annual cost, \$ year^{-1}

Greek

α	—	Transfer coefficient/annualized factor
β	—	Maintenance factor
ψ_{em}	—	Penalty price for emission, \$ kg^{-1}
ε	—	Effectiveness
ϕ_f	—	Unit price of fuel, \$ kg^{-1}
ΔP	—	Pressure drop, Pa
η	—	Efficiency or effectiveness

Subscripts

c	—	Cold
cs	—	Condensate
D	—	Distilled, diesel engine
e	—	Exit condition
f	—	Fuel, feed
i, j	—	Counter
in	—	Inlet condition
net	—	Total net power
nom	—	Nominal
°	—	Reference ambient condition
out	—	Outlet condition
P	—	Pump and product or concentrated
reg	—	Regenerator
s	—	Steam state
v	—	Vapor state

Acknowledgments

This work was supported by the National Research Foundation of Korea (NRF) grant funded by the Korean government (MSIT) through GCRC-SOP (No. 2011-0030013).

References

[1] S.M. Shalaby, Reverse osmosis desalination powered by photovoltaic and solar Rankine cycle power systems: a review, Renewable Sustainable Energy Rev., 73 (2017) 789–797.
[2] M.A. Abdelkareem, M. El Haj Assad, E.T. Sayed, B. Soudan, Recent progress in the use of renewable energy sources to power water desalination plants, Desalination, 435 (2018) 97–113.
[3] P. Pouyfaucon, A. Buenaventura, L. García-Rodríguez, Solar thermal-powered desalination: a viable solution for a potential market, Desalination, 435 (2018) 60–69.
[4] M. Yari, L. Ariyanfar, E. Abdi Aghdam, Analysis and performance assessment of a novel ORC based multi-generation system for power, distilled water and heat, Renewable Energy, 119 (2018) 262–281.
[5] L. Ariyanfar, M. Yari, E. Abdi Aghdam, Proposal and performance assessment of novel combined ORC and HDD cogeneration systems, Appl. Therm. Eng., 108 (2016) 296–311.
[6] W.F. He, C. Ji, D. Han, Y.K. Wu, L. Huang, X.K. Zhang, Performance analysis of the mechanical vapor compression desalination system driven by an organic Rankine cycle, Energy, 141 (2017) 1177–1186.
[7] M.A. Al-Weshahi, A. Anderson, G. Tian, Organic Rankine cycle recovering stage heat from MSF desalination distillate water, Appl. Energy, 130 (2014) 738–747.
[8] V.G. Gude, Use of exergy tools in renewable energy driven desalination systems, Therm. Sci. Eng. Prog., 8 (2018) 154–170.
[9] M.L. Elsayed, O. Mesalhy, R.H. Mohammed, L.C. Chow, Exergy and thermo-economic analysis for MED-TVC desalination systems, Desalination, 447 (2018) 29–42.
[10] L. Savvina, H.A. Arafat, Techno-economic analysis of MED and RO desalination powered by low-enthalpy geothermal energy, Desalination, 365 (2015) 277–292.
[11] J. Bundschuh, N. Ghaffour, H. Mahmoudi, M. Goosen, S. Mushtaq, J. Hoinkis, Low-cost low-enthalpy geothermal heat for freshwater production: innovative applications using thermal desalination processes, Renewable Sustainable Energy Rev., 43 (2015) 196–206.
[12] J. Nihill, A. Date, P. Lappas, J. Velardo, Investigating the prospects of water desalination using a thermal water pump coupled with reverse osmosis membrane, Desalination, 445 (2018) 256–265.

[13] Z. Hajabdollahi, F. Hajabdollahi, M. Tehrani, H. Hajabdollahi, Thermo-economic environmental optimization of organic Rankine Cycle for diesel waste heat recovery, Energy, 63 (2013) 142–151.
[14] B. Ortega-Delgado, P. Palenzuela, D.C. Alarcón-Padilla, Parametric study of a multi-effect distillation plant with thermal vapor compression for its integration into a Rankine cycle power block, Desalination, 394 (2016) 18–29.
[15] S. Sadri, M. Ameri, R.H. Khoshkhoo, Multi-objective optimization of MED-TVC-RO hybrid desalination system based on the irreversibility concept, Desalination, 402 (2017) 97–108.
[16] J.C. Bruno, J. Lopez-Villada, E. Letelier, S. Romera, A. Coronas, Modelling and optimisation of solar organic Rankine cycle engines for reverse osmosis desalination, Appl. Therm. Eng., 28 (2008) 2212–2226.
[17] D. Manolakos, G. Kosmadakis, S. Kyritsis, G. Papadakis, Identification of behaviour and evaluation of performance of small scale, low-temperature organic Rankine cycle system coupled with a RO desalination unit, Energy, 6 (2009) 767–774.
[18] K. Deb, T. Goel, Controlled Elitist Non-dominated Sorting Genetic Algorithms for Better Convergence, International Conference on Evolutionary Multi-Criterion Optimization, Berlin, Heidelberg, 2001, pp. 67–81.
[19] K. Deb, A. Pratap, S. Agarwal, T. Meyarivan, A fast and elitist multiobjective genetic algorithm: NSGA-II, IEEE Trans. Evol. Comput., 2 (2002) 182–197.
[20] S. Khalilzadeh, A.H. Nezhad, Utilization of waste heat of a high-capacity wind turbine in multi effect distillation desalination: energy, exergy and thermoeconomic analysis, Desalination, 439 (2018) 119–137.
[21] P.L. Yu, Multiple-Criteria Decision Making: Concepts, Techniques, and Extensions, Vol. 30, Springer Science & Business Media, University of Kansas, Kansas, 2013, pp. 21–53.
[22] F. Hajabdollahi, Z. Hajabdollahi, H. Hajabdollahi, Soft computing based multi-objective optimization of steam cycle power plant using NSGA-II and ANN, Appl. Soft Comput., 11 (2012) 3648–3655.